

# Optimal Clustering under Uncertainty

Lori A. Dalton, Marco E. Benalcázar, and Edward R. Dougherty

## Abstract

Classical clustering algorithms typically either lack an underlying probability framework to make them predictive or focus on parameter estimation rather than defining and minimizing a notion of error. Recent work addresses these issues by developing a probabilistic framework based on the theory of random labeled point processes and characterizing a *Bayes clusterer* that minimizes the number of misclustered points. The Bayes clusterer is analogous to the Bayes classifier. Whereas determining a Bayes classifier requires full knowledge of the feature-label distribution, deriving a Bayes clusterer requires full knowledge of the point process. When uncertain of the point process, one would like to find a robust clusterer that is optimal over the uncertainty, just as one may find optimal robust classifiers with uncertain feature-label distributions. Herein, we derive an optimal robust clusterer by first finding an *effective* random point process that incorporates all randomness within its own probabilistic structure and from which a Bayes clusterer can be derived that provides an optimal robust clusterer relative to the uncertainty. This is analogous to the use of effective class-conditional distributions in robust classification. After evaluating the performance of robust clusterers in synthetic mixtures of Gaussians models, we apply the framework to granular imaging, where we make use of the asymptotic granulometric moment theory for granular images to relate robust clustering theory to the application.

## Index Terms

Clustering, Bayesian robustness; granular imaging; small samples.

## I. INTRODUCTION

The basic optimization paradigm for operator design consists of four parts: (1) define the underlying random process; (2) define the class of potential operators; (3) characterize operator performance via a cost function; and (4) find an operator to minimize the cost function. The classic example is the Wiener filter, where the four parts consist of wide-sense stationary true and observed signals, linear operators, minimization of the mean-square error, and optimization in terms of power spectra. In practice, we might be uncertain as to the distribution governing the random process so that we desire a *robust* operator, one whose performance is acceptable relative to the uncertainty. Robust design can be posed in the following way: Given a class of operators and given that the *state of nature* is uncertain but contained in some *uncertainty class*, which operator should be selected to optimize performance across all possible states of nature?

Our interest here is in clustering, where the underlying process is a random point set and the aim is to partition the point set into clusters corresponding to the manner in which the points have been generated by the underlying process. Having developed the theory of optimal clustering in the context of random labeled point sets where optimality is with respect to mis-clustered points [1], we now consider optimal clustering when the underlying random labeled point process belongs to an uncertainty class of random labeled point processes, so that optimization is relative to both clustering error and model uncertainty. This is analogous to finding an optimal Wiener filter when the signal process is unknown, so that the

L. A. Dalton is with the Department of Electrical and Computer Engineering, The Ohio State University, Columbus, OH 43210 USA (e-mail: dalton.lori@outlook.com).

M. E. Benalcázar is with the Secretaría Nacional de Educación Superior, Ciencia, Tecnología e Innovación (SENESCYT), Ecuador, the Consejo Nacional de Investigaciones Científicas y Técnicas (CONICET), Argentina, the Facultad de Ingeniería, Universidad Nacional de Mar del Plata, Mar del Plata, Argentina, and the Escuela Politécnica Nacional, Departamento de Informática y Ciencias de la Computación, Quito, Ecuador (e-mail: marco\_benalcazar@hotmail.com).

E. R. Dougherty is with the Department of Electrical and Computer Engineering, Texas A&M University, College Station, TX 77843 USA (e-mail: edward@ece.tamu.edu).

power spectra belong to an uncertainty class [2]. We now briefly review classical robust operator theory, which will serve as the foundation for a new general theory of optimal robust clustering.

Optimal robust filtering first appeared in signal processing in the 1970s when the problem was addressed for signals with uncertain power spectra. Early work considered robust filter design from a minimax perspective: the filter is designed for the state having the best worst-case performance over all states [3], [4], [5]. Whereas the standard optimization problem given certainty with regard to the random process takes the form

$$\psi^* = \arg \min_{\psi \in \mathcal{C}} \gamma(\psi), \quad (1)$$

where  $\mathcal{C}$  is the operator class and  $\gamma(\psi)$  is the cost of applying operator  $\psi$  on the model, minimax optimization is defined by

$$\psi_{\text{MM}} = \arg \min_{\psi \in \mathcal{C}_\Theta} \max_{\theta \in \Theta} \gamma_\theta(\psi), \quad (2)$$

where  $\Theta$  is the uncertainty class of random processes,  $\mathcal{C}_\Theta$  is the class of operators that are optimal for some state in the uncertainty class, and  $\gamma_\theta(\psi)$  is the cost of applying operator  $\psi$  for state  $\theta \in \Theta$ .

Suppose one has prior knowledge with which to construct a prior distribution  $\pi(\theta)$  on states (models) in the uncertainty class. Rather than apply a minimax robust operator, whose average performance can be poor, a Bayesian approach can be taken whereby optimization is relative to  $\pi(\theta)$ . A *model-constrained (state-constrained) Bayesian robust (MCBR) operator* minimizes the expected error over the uncertainty class among all operators in  $\mathcal{C}_\Theta$ :

$$\psi_{\text{MCBR}} = \arg \min_{\psi \in \mathcal{C}_\Theta} E_\theta[\gamma_\theta(\psi)]. \quad (3)$$

MCBR filtering has been considered for morphological, binary and linear filtering. MCBR design has also been applied in classification with uncertain feature-label distributions [6].

Rather than restrict optimization to operators that are optimal for some state in the uncertainty class, one can optimize over any class of operators, including unconstrained optimization over all possible measurable functions. In this case, the optimal operator is called an *intrinsically optimal Bayesian robust (IBR) operator (filter)* and (3) becomes

$$\psi_{\text{IBR}} = \arg \min_{\psi \in \mathcal{C}} E_\theta[\gamma_\theta(\psi)], \quad (4)$$

where  $\mathcal{C}$  is a set of operators under consideration. IBR filtering has been considered for linear and morphological filtering [2]. The IBR approach was first used to design optimal classifiers when the unknown true feature-label distribution belongs to an uncertainty class [7], [8]. In that setting, optimization is relative to a posterior distribution obtained from the prior utilizing sample data and an optimal classifier is called an *optimal Bayesian classifier (OBC)*.

Unlike the state of affairs in filtering and classification, classical clustering algorithms typically lack an underlying probability framework to make them predictive. The exceptions, for instance, expectation-maximization based on mixture models, typically focus on parameter estimation rather than defining and minimizing a notion of operator error. Work in [9] and [1] addresses the solution to (1) in the context of clustering using a probabilistic theory of clustering for random labeled point sets and a definition of clustering error given by the expected number of “misclustered” points. This results in a *Bayes clusterer*, which minimizes error under the assumed probabilistic framework. An (optimal) Bayes clusterer is analogous to an (optimal) *Bayes classifier*, which minimizes classification error under the assumed feature-label distribution. Here, we characterize robust clustering using the framework and definitions of error in [9] and [1], and introduce definitions of robust clustering that parallel concepts from filtering. In particular, we present minimax, MCBR and IBR clusterers, and develop effective stochastic processes for robust clustering. We also evaluate performance under mixtures of Gaussians and demonstrate how the methodology can be implemented in practice with an example from granular imaging.

## II. BAYES CLUSTERING THEORY

In this section, we review Bayes clustering theory from [9] and [1]. A *random labeled point process* (RLPP) is characterized by a pair,  $(\Xi, \Lambda)$ , where  $\Xi$  is a point process generating a point set  $S \subset \mathbb{R}^d$  and  $\Lambda$  generates random labels on the points in  $S$ . In particular, let  $\eta(S)$  denote the number of points in  $S$ . The first component in this pair,  $\Xi$ , maps from a probability space to  $(\mathbf{N}, \mathcal{N})$ , where  $\mathbf{N}$  is the family of finite sequences in  $\mathbb{R}^d$  and  $\mathcal{N}$  is the smallest  $\sigma$ -algebra on  $\mathbf{N}$  such that for any Borel set  $B$  in  $\mathbb{R}^d$  the mapping  $S \mapsto \eta(S \cap B)$  is measurable. A probability measure,  $\nu$ , of  $\Xi$  is determined by the probabilities  $\nu(Y)$  for  $Y \in \mathcal{N}$ , or (via the Choquet-Matheron-Kendall theorem [10], [11], [12], [13]), may be reduced to the system of probabilities  $P(\Xi \cap K \neq \emptyset)$  over all compact sets  $K \subseteq \mathbb{R}^d$ . Given a point set  $S \in \mathbf{N}$ , a label function  $\phi_S : S \rightarrow L = \{1, 2, \dots, l\}$  is a deterministic mapping that assigns each point  $\mathbf{x} \in S$  to label  $\phi_S(\mathbf{x}) \in L$ . The second component,  $\Lambda$ , is a random labeling, that is,  $\Lambda = \{\Phi_S : S \in \mathbf{N}\}$ , where  $\Phi_S$  is a random label function with probability mass  $P(\Phi_S = \phi_S | S)$  on  $L^S$ .

For any set  $S$ , and pair of label functions  $\phi_S$  and  $\varphi_S$ , define the *label mismatch error* between  $\phi_S$  and  $\varphi_S$  to be the proportion of points where the label functions differ:

$$\varepsilon(S, \phi_S, \varphi_S) = \frac{1}{\eta(S)} \sum_{\mathbf{x} \in S} I_{\phi_S(\mathbf{x}) \neq \varphi_S(\mathbf{x})}, \quad (5)$$

where  $I_A$  is an indicator function equal to 1 if  $A$  is true and 0 otherwise. Clustering involves identifying partitions of a point set rather than the actual labeling. A partition of  $S$  into  $l$  clusters has the form  $\mathcal{P}_S = \{S_1, S_2, \dots, S_l\}$  such that the  $S_y$  are disjoint and  $S = \bigcup_{y=1}^l S_y$ . Every partition  $\mathcal{P}_S$  has associated with it a family,  $G_{\mathcal{P}_S}$ , of label functions that induce the partition  $\mathcal{P}_S$ . That is,  $\varphi_S \in G_{\mathcal{P}_S}$  if and only if  $\mathcal{P}_S = \{S_1, S_2, \dots, S_l\}$  where  $S_y = \{\mathbf{x} \in S : \varphi_S(\mathbf{x}) = l_y\}$  and  $(l_1, \dots, l_l)$  is a permutation of  $L$ . For any point set  $S$ , label function  $\phi_S$ , and partition  $\mathcal{P}_S$ , define the *cluster mismatch error* to be the minimum label mismatch error between  $\phi_S$  and all label functions that induce  $\mathcal{P}_S$ :

$$\varepsilon(S, \phi_S, \mathcal{P}_S) = \min_{\varphi_S \in G_{\mathcal{P}_S}} \varepsilon(S, \phi_S, \varphi_S). \quad (6)$$

This is a simplified version of the original definition in [9]. Define the *partition error* of  $\mathcal{P}_S$  to be the mean cluster mismatch error over the distribution of label functions on  $S$ :

$$\begin{aligned} \varepsilon(S, \mathcal{P}_S) &= E_{\Phi_S}[\varepsilon(S, \Phi_S, \mathcal{P}_S) | S] \\ &= E_{\Phi_S} \left[ \min_{\varphi_S \in G_{\mathcal{P}_S}} \varepsilon(S, \Phi_S, \varphi_S) \middle| S \right]. \end{aligned} \quad (7)$$

In [1], it was shown that (7) can be written in the form

$$\varepsilon(S, \mathcal{P}_S) = \sum_{\mathcal{Q}_S \in \mathcal{K}_S} c_S(\mathcal{P}_S, \mathcal{Q}_S) P_S(\mathcal{Q}_S), \quad (8)$$

where  $\mathcal{K}_S$  is the set of all partitions of  $S$ ,

$$P_S(\mathcal{Q}_S) = \sum_{\phi_S \in G_{\mathcal{Q}_S}} P(\Phi_S = \phi_S | S) \quad (9)$$

is the probability mass function on partitions  $\mathcal{Q}_S \in \mathcal{K}_S$  of  $S$ , and we define the *natural partition cost function*,

$$c_S(\mathcal{P}_S, \mathcal{Q}_S) = \frac{1}{\eta(S)} \min_{\varphi_S \in G_{\mathcal{P}_S}, \phi_S \in G_{\mathcal{Q}_S}} \sum_{\mathbf{x} \in S} I_{\phi_S(\mathbf{x}) \neq \varphi_S(\mathbf{x})}. \quad (10)$$

The partition error under the natural cost function is essentially the average number of misclustered points.

Taking (8) as a generalized definition, other cost functions can be applied [14], [15], [16], [17]. The natural cost function stands out in two respects. First, while these works define loss over label functions, we define cost directly over partitions, which is mathematically cleaner, and automatically treats the label

switching problem in which multiple distinct label functions may produce the same partitions. Second, these works treat loss abstractly without connecting to a practical notion of clustering error, like the expected (minimum) number of mislabeled points. In contrast, we begin with a practical definition of clustering error, and show that minimizing clustering error equivalently minimizes (8) relative to the natural cost function.

Let  $\mathcal{C}_S = \{\mathcal{P}_S^1, \dots, \mathcal{P}_S^c\} \subseteq \mathcal{K}_S$  be a set of  $c$  candidate partitions that comprise the search space and  $\mathcal{R}_S = \{\mathcal{Q}_S^1, \dots, \mathcal{Q}_S^r\} \subseteq \mathcal{K}_S$  be a set of  $r$  reference partitions with known probabilities. The partition error of all candidate partitions may be found via

$$\begin{aligned} & [\varepsilon(S, \mathcal{P}_S^1) \ \cdots \ \varepsilon(S, \mathcal{P}_S^c)]^T \\ &= \begin{bmatrix} c_S(\mathcal{Q}_S^1, \mathcal{P}_S^1) & \cdots & c_S(\mathcal{Q}_S^r, \mathcal{P}_S^1) \\ \vdots & \ddots & \vdots \\ c_S(\mathcal{Q}_S^1, \mathcal{P}_S^c) & \cdots & c_S(\mathcal{Q}_S^r, \mathcal{P}_S^c) \end{bmatrix} \begin{bmatrix} P_S(\mathcal{Q}_S^1) \\ \vdots \\ P_S(\mathcal{Q}_S^r) \end{bmatrix}, \end{aligned} \quad (11)$$

where  $T$  denotes matrix transpose. Given  $S$ , setting  $\mathcal{C}_S = \mathcal{R}_S = \mathcal{K}_S$  requires a cost matrix of size  $|\mathcal{K}_S| \times |\mathcal{K}_S|$ , which can be prohibitively large for moderate  $\eta(S)$ . To alleviate this, [1] provides both exact and approximate techniques to evaluate (11) under the natural cost function with reduced complexity.

A cluster operator  $\zeta$  maps point sets to partitions. Define the *clustering error* of cluster operator  $\zeta$  to be the mean partition error of  $\zeta(\Xi)$  over the random point sets  $\Xi$ :

$$\varepsilon(\zeta) = E_{\Xi}[\varepsilon(\Xi, \zeta(\Xi))].$$

A *Bayes cluster operator*  $\zeta^*$  is a clusterer having minimal clustering error  $\varepsilon(\zeta^*)$ , which is called the *Bayes clustering error*. Since  $\varepsilon(\zeta) = E_{\Xi}[\varepsilon(\Xi, \zeta(\Xi))]$  and  $\varepsilon(S, \zeta(S))$  depends on the clusterer  $\zeta$  only at point set  $S$ ,  $\varepsilon(\zeta)$  is minimized by setting  $\zeta^*(S) = \mathcal{P}_S^*$  for all  $S \in \mathbf{N}$ , where  $\mathcal{P}_S^*$  is a *Bayes partition* of  $S$ , defined to be a partition having minimal partition error,  $\varepsilon(S, \mathcal{P}_S^*)$ , called the *Bayes partition error*.

This formulation parallels classification theory, where an RLPP corresponds to a feature-label distribution,  $\varepsilon(S, \mathcal{P}_S)$  corresponds to the probability that a given label is incorrect for a fixed point in the feature space,  $\varepsilon(\zeta)$  corresponds to the overall classification error for an arbitrary classifier,  $\zeta^*$  corresponds to a Bayes classifier, and  $\varepsilon(\zeta^*)$  corresponds to the Bayes classification error.

### A. Separable RLPPs

Up to this point, we have characterized RLPPs with a point process  $\Xi$  that generates point sets,  $S$ , followed by an  $S$ -conditioned labeling process  $\Lambda$  that generates label functions,  $\phi_S$ . Alternatively, it is often easier to characterize an RLPP as a process that draws a sample size  $n$ , a set of labels for  $n$  points, and a set of  $n$  points with distributions corresponding to the labels. For instance, one might think of points being drawn from  $l$  Gaussian distributions possessing random parameters. We say that an RLPP is *separable* if a label function  $\phi$  is generated from an independent label generating process  $\Phi$  with probability mass function  $P(\Phi = \phi)$  over the set of all label functions with domain  $\{1, 2, \dots, n\}$ , a random parameter vector  $\rho$  is independently drawn from a distribution  $f(\rho)$ , and the  $i$ th point  $\mathbf{x}_i$  in  $S$ , with corresponding label  $y = \phi(i)$ , is independently drawn from a conditional distribution  $f(\mathbf{x}|y, \rho)$ . From Bayes rule, the probability of label function  $\phi_S \in L^S$  given  $S = \{\mathbf{x}_1, \dots, \mathbf{x}_n\}$  is

$$P(\Phi_S = \phi_S | S) \propto f(S|\phi)P(\Phi = \phi), \quad (12)$$

where  $\phi(i) = \phi_S(\mathbf{x}_i)$ ,

$$f(S|\phi) = \int \left( \prod_{y=1}^l \prod_{\mathbf{x} \in S_y} f(\mathbf{x}|y, \rho) \right) f(\rho) d\rho, \quad (13)$$

and  $S_y = \{\mathbf{x}_i : \phi(i) = y, i = 1, \dots, n\}$  is the set of points in  $S$  assigned label  $y$ . A separable RLPP thus has three components:  $P(\Phi = \phi)$ ,  $f(\rho)$  and  $f(\mathbf{x}|y, \rho)$ , where  $P(\Phi = \phi)$  is a prior on labels, which is

not dependent on  $S$ , and  $P(\Phi_S = \phi_S|S)$  is a posterior probability on labels given a specific point set  $S$ , which is found using (12) and (13).

If  $\rho = [\rho_1, \dots, \rho_l]$ , where the  $\rho_y$  are mutually independent parameter vectors and the label- $y$ -conditional distribution depends on only  $\rho_y$ , that is, if  $f(\mathbf{x}|y, \rho) = f(\mathbf{x}|y, \rho_y)$  for  $y = 1, \dots, l$ , then,

$$f(S|\phi) = \prod_{y=1}^l \int \left( \prod_{\mathbf{x} \in S_y} f(\mathbf{x}|y, \rho_y) \right) f(\rho_y) d\rho_y. \quad (14)$$

### B. Gaussian RLPPs

Expressions for label function probabilities have been solved under several models in [1]. Here, we review an important case in which clusters are Gaussian with random means and covariances. Specifically, consider a separable RLPP where, for each  $y \in \{1, \dots, l\}$ ,  $\rho_y = [\mu_y, \Sigma_y]$  and  $f(\mathbf{x}|y, \rho_y)$  is a Gaussian distribution with mean  $\mu_y$  and covariance  $\Sigma_y$ . Given a label function  $\phi_S$ , let  $y \in \{1, \dots, l\}$  be fixed, and let  $n_y$  be the number of points in  $S$  assigned label  $y$ . For  $n_y \geq 2$  it was shown in [1] that

$$\prod_{\mathbf{x} \in S_y} f(\mathbf{x}|y, \rho_y) = (2\pi)^{-\frac{dn_y}{2}} |\Sigma_y|^{-\frac{n_y}{2}} \exp\left(-\frac{1}{2} \text{tr}(\Phi_y^* \Sigma_y^{-1})\right), \quad (15)$$

where  $|\cdot|$  is a determinant,  $\text{tr}(\cdot)$  is a trace,

$$\Phi_y^* = (n_y - 1) \widehat{\Sigma}_y + n_y (\mu_y - \widehat{\mu}_y) (\mu_y - \widehat{\mu}_y)^T,$$

and  $\widehat{\mu}_y$  and  $\widehat{\Sigma}_y$  are the sample mean and covariance of points in  $S_y$ , respectively. When  $n_y = 1$ , (15) holds with  $\Phi_y^* = (\mu_y - \widehat{\mu}_y) (\mu_y - \widehat{\mu}_y)^T$ , and when  $n_y = 0$  the product over an empty set is 1.

Assume  $f(\rho_y) = f(\Sigma_y) f(\mu_y|\Sigma_y)$ , where  $f(\mu_y|\Sigma_y)$  is a Gaussian distribution with mean  $\mathbf{m}_y$  and covariance  $\frac{1}{\nu_y} \Sigma_y$  with  $\nu_y > 0$ , and  $f(\Sigma_y)$  is an inverse-Wishart distribution with  $\kappa_y > d - 1$  degrees of freedom and a positive-definite scale matrix  $\Psi_y$ , i.e.,

$$f(\Sigma_y) = \frac{|\Psi_y|^{\frac{\kappa_y}{2}} |\Sigma_y|^{-\frac{\kappa_y+d+1}{2}}}{2^{\frac{\kappa_y d}{2}} \Gamma_d(\frac{\kappa_y}{2})} \exp\left(-\frac{1}{2} \text{tr}(\Psi_y \Sigma_y^{-1})\right),$$

where  $\Gamma_d$  is the multivariate Gamma function. The expected mean is  $\mathbf{m}_y$ , the expected covariance matrix is  $\frac{1}{\kappa_y - d - 1} \Psi_y$  if  $\kappa_y > d + 1$ , and as  $\nu_y$  and  $\kappa_y$  increase  $f(\rho_y)$  becomes more ‘‘informative.’’ The probability of label function  $\phi_S$  under this RLPP is found from (12) and (14) as

$$P(\Phi_S = \phi_S|S) \propto P(\Phi = \phi) \prod_{y=1}^l \frac{\Gamma_d(\frac{\kappa_y + n_y}{2})}{|n_y + \nu_y|^{\frac{d}{2}} |\Psi_y + \Psi_y^*|^{\frac{\kappa_y + n_y}{2}}}, \quad (16)$$

where

$$\Psi_y^* = (n_y - 1) \widehat{\Sigma}_y + \frac{\nu_y n_y}{\nu_y + n_y} (\widehat{\mu}_y - \mathbf{m}_y) (\widehat{\mu}_y - \mathbf{m}_y)^T \quad (17)$$

for  $n_y = 2$ ,  $\Psi_y^* = \frac{\nu_y}{\nu_y + 1} (\widehat{\mu}_y - \mathbf{m}_y) (\widehat{\mu}_y - \mathbf{m}_y)^T$  for  $n_y = 1$ , and  $\Psi_y^* = 0$  for  $n_y = 0$ . If  $\nu_1 = \dots = \nu_l$ ,  $\kappa_1 = \dots = \kappa_l$  and  $P(\Phi = \phi)$  is such that the size of each cluster is fixed and partitions with clusters of the specified sizes are equally likely, then for any  $\phi_S$  inducing clusters of the correct sizes,

$$P(\Phi_S = \phi_S|S) \propto \prod_{y=1}^l |\Psi_y + \Psi_y^*|^{-\frac{\kappa_y + n_y}{2}}. \quad (18)$$

Similar derivations for the posterior on parameters under Gaussian mixture models can be found in [18], and on label functions under Gaussian mixture models can be found in [14].

### III. ROBUST CLUSTERING OPERATORS

Under a known RLPP  $(\Xi, \Lambda)$ , optimization in the Bayes clusterer is over the set  $\bar{\mathcal{C}}$  of all clustering algorithms with respect to the clustering error,

$$\zeta^* = \arg \min_{\zeta \in \bar{\mathcal{C}}} \varepsilon(\zeta); \quad (19)$$

however, in practice the RLPP is likely to be uncertain. In this section we present definitions for optimal Bayesian robust clustering and show that IBR clusterers solve an optimization problem of the same form as in (19) under an effective process.

#### A. Definitions of Robust Clustering

We present three robust clustering operators: minimax robust clustering, model-constrained Bayesian robust (MCBR) clustering, and intrinsically optimal Bayesian robust (IBR) clustering. Our main interest is in IBR clustering. The first two methods are provided to emphasize parallels between the new theory and existing robust operator theory from filtering and classification.

Consider a parameterized uncertainty class of RLPPs  $(\Xi_\theta, \Lambda_\theta)$ ,  $\theta \in \Theta$ , where  $\Xi_\theta$  is a point process on  $(\mathbf{N}, \mathcal{N})$ ,  $\Lambda_\theta = \{\Phi_{\theta,S} : S \in \mathbf{N}\}$  is a random labeling on  $\mathbf{N}$  consisting of a random label function  $\Phi_{\theta,S}$  for each  $S$ , and  $\varepsilon_\theta(\zeta)$  is the error of cluster operator  $\zeta$  for state  $\theta$ .

A *minimax robust clusterer*  $\zeta_{\text{MM}}$  is defined by (2) with  $\mathcal{C}_\Theta$  being the set of state-specific Bayes clusterers and  $\varepsilon_\theta(\zeta)$  in place of  $\gamma_\theta(\psi)$ . An *MCBR cluster operator*  $\zeta_{\text{MCBR}}$  is defined by (3) with  $\varepsilon_\theta(\zeta)$  in place of  $\gamma_\theta(\psi)$ .

Our focus is on optimization over the full class  $\bar{\mathcal{C}}$  of cluster operators. This yields an *IBR cluster operator*,

$$\zeta_{\text{IBR}} = \arg \min_{\zeta \in \bar{\mathcal{C}}} E_\theta[\varepsilon_\theta(\zeta)]. \quad (20)$$

In analogy to [2], where effective characteristics for IBR linear filtering were derived from effective random signal processes, here we show how IBR cluster operators can be found via effective random labeled point processes.

#### B. Effective Random Labeled Point Processes

We begin with two definitions.

**Definition 1.** An RLPP is solvable under clusterer class  $\mathcal{C}$  if

$$\zeta^* = \arg \min_{\zeta \in \mathcal{C}} \varepsilon(\zeta)$$

can be solved under this process.

**Definition 2.** Let  $\Theta$  be an uncertainty class of RLPPs having prior  $\pi(\theta)$ . An RLPP  $(\Xi_{\text{eff}}, \Lambda_{\text{eff}})$  is an effective RLPP under clusterer class  $\mathcal{C}$  if for all  $\zeta \in \mathcal{C}$  both the expected clustering error  $E_\theta[\varepsilon_\theta(\zeta)]$  under the uncertainty class of RLPPs and the clustering error  $\varepsilon_{\text{eff}}(\zeta)$  under  $(\Xi_{\text{eff}}, \Lambda_{\text{eff}})$  exist and

$$E_\theta[\varepsilon_\theta(\zeta)] = \varepsilon_{\text{eff}}(\zeta). \quad (21)$$

**Theorem 1.** Let  $\Theta$  parameterize an uncertainty class of RLPPs with prior  $\pi(\theta)$ . If there exists a solvable effective RLPP  $(\Xi_{\text{eff}}, \Lambda_{\text{eff}})$  under clusterer class  $\mathcal{C}$  with optimal clusterer  $\zeta_{\text{eff}}^*$ , then  $\zeta_{\text{eff}}^* = \arg \min_{\zeta \in \mathcal{C}} E_\theta[\varepsilon_\theta(\zeta)]$ . If  $\mathcal{C} = \mathcal{C}_\Theta$ , then  $\zeta_{\text{MCBR}}^* = \zeta_{\text{eff}}^*$ , and if  $\mathcal{C} = \bar{\mathcal{C}}$ , then  $\zeta_{\text{IBR}}^* = \zeta_{\text{eff}}^*$ .

*Proof.* The proof is immediate from the definition of an effective RLPP and (19):

$$\arg \min_{\zeta \in \mathcal{C}} E_\theta[\varepsilon_\theta(\zeta)] = \arg \min_{\zeta \in \mathcal{C}} \varepsilon_{\text{eff}}(\zeta) = \zeta_{\text{eff}}^*.$$

The solutions for MCBR and IBR clustering follow from their definitions.  $\square$

To find an MCBR or IBR clusterer, we first seek an effective RLPP. This effective RLPP is not required to be a member of the uncertainty class parameterized by  $\theta$ , but must be solvable. If  $(\Xi_{\text{eff}}, \Lambda_{\text{eff}})$  is an effective RLPP under clusterer class  $\mathcal{C}$ , then it is an effective RLPP under any smaller clusterer class. Hence, an effective RLPP found for IBR clustering is also an effective RLPP for MCBR clustering. However, not only are IBR clusterers better performing than MCBR clusterers, they are typically much easier to find analytically. In particular, the IBR clusterer is directly solved by importing methods from Bayes clustering theory, i.e., one may solve (19) by minimizing the partition error over all partitions of a point set  $S$  under the effective RLPP. The MCBR clusterer, on the other hand, is significantly hampered by computational overhead in finding  $\mathcal{C}_\Theta$  and actually evaluating the clustering error for each  $\zeta \in \mathcal{C}_\Theta$ . The next theorem addresses the existence of effective RLPPs.

**Theorem 2.** *Let  $\Theta$  parameterize an uncertainty class  $\{(\Xi_\theta, \Lambda_\theta)\}_{\theta \in \Theta}$  of RLPPs with prior  $\pi(\theta)$ . There exists an RLPP,  $(\Xi_{\text{eff}}, \Lambda_{\text{eff}})$ , such that*

$$E_\theta [E_{\Xi_\theta, \Lambda_\theta} [g(\Xi_\theta, \Phi_{\theta, \Xi_\theta}) | \theta]] = E_{\Xi_{\text{eff}}, \Lambda_{\text{eff}}} [g(\Xi_{\text{eff}}, \Phi_{\text{eff}, \Xi_{\text{eff}}})] \quad (22)$$

for any real-valued measurable function,  $g$ .

*Proof.* Suppose that the parameter  $\theta$  is a realization of a random vector,  $\vartheta : (\Omega, \mathcal{A}, P) \rightarrow (\Theta, \mathcal{B})$ . Then  $\{\vartheta^{-1}(\theta) : \theta \in \Theta\}$  partitions the sample space,  $\Omega$ . The point process  $\Xi_\theta$  is thus a mapping

$$\Xi_\theta : (\vartheta^{-1}(\theta), \mathcal{A} \cap \vartheta^{-1}(\theta), P_\theta) \rightarrow (\mathbf{N}, \mathcal{N}),$$

where  $P_\theta$  is the conditional probability and we assume  $\nu_\theta(Y) = P_\theta(\Xi_\theta^{-1}(Y))$  for all  $Y \in \mathcal{N}$  is known. Write the random labeling as  $\Lambda_\theta = \{\Phi_{\theta, S} : S \in \mathbf{N}\}$ , where  $\Phi_{\theta, S}$  has a probability mass function  $P(\Phi_{\theta, S} = \phi_S | \theta, S)$  on  $L^S$ . Given any real-valued measurable function  $g$  mapping from point set and label function pairs, let  $X = g(\Xi, \Phi_\Xi)$  be a random variable where  $(\Xi, \Phi_\Xi)$  is drawn from  $\{(\Xi_\theta, \Lambda_\theta)\}_{\theta \in \Theta}$  with prior  $\pi(\theta)$ , and note  $E_\theta[E[X|\theta]] = E[X]$ .

Let  $\Xi_{\text{eff}} : (\Omega, \mathcal{A}, P) \rightarrow (\mathbf{N}, \mathcal{N})$  be a mapping, where given a fixed  $\omega \in \Omega$  we have a corresponding fixed realization  $\theta = \vartheta(\omega)$  and we define  $\Xi_{\text{eff}}(\omega) = \Xi_\theta(\omega)$ . Note that

$$\nu(Y) \equiv P(\Xi_{\text{eff}}^{-1}(Y)) = E_\theta[\nu_\theta(Y)]$$

and  $\Xi_{\text{eff}}$  is a random point process. Define  $\Lambda_{\text{eff}} = \{\Phi_{\text{eff}, S} : S \in \mathbf{N}\}$ , where  $\Phi_{\text{eff}, S}$  has a probability mass function

$$P(\Phi_{\text{eff}, S} = \phi_S | S) = E_\theta[P(\Phi_{\theta, S} = \phi_S | \theta, S)]$$

for all  $\phi_S \in L^S$ . Thus,  $\Lambda_{\text{eff}}$  is a random labeling. Let  $Z = g(\Xi_{\text{eff}}, \Phi_{\text{eff}, \Xi_{\text{eff}}})$  be a random variable where  $(\Xi_{\text{eff}}, \Phi_{\text{eff}, \Xi_{\text{eff}}})$  is drawn from the RLPP we have constructed,  $(\Xi_{\text{eff}}, \Lambda_{\text{eff}})$ , and note  $E[X] = E[Z]$ .  $\square$

Theorem 2 applies for any function  $g(S, \phi_S)$ , including the cluster mismatch error  $g(S, \phi_S) = \varepsilon(S, \phi_S, \zeta(S))$ , for any clusterer  $\zeta \in \bar{\mathcal{C}}$ . Thus, (22) implies

$$\begin{aligned} E_\theta [\varepsilon_\theta(\zeta)] &= E_\theta [E_{\Xi_\theta, \Lambda_\theta} [\varepsilon(\Xi_\theta, \Phi_{\theta, \Xi_\theta}, \zeta(\Xi_\theta)) | \theta]] \\ &= E_{\Xi_{\text{eff}}, \Lambda_{\text{eff}}} [\varepsilon(\Xi_{\text{eff}}, \Phi_{\text{eff}, \Xi_{\text{eff}}}, \zeta(\Xi_{\text{eff}}))] = \varepsilon_{\text{eff}}(\zeta). \end{aligned}$$

Hence,  $(\Xi_{\text{eff}}, \Lambda_{\text{eff}})$  is an effective RLPP on  $\bar{\mathcal{C}}$ , covering MCBR and IBR clusterers.

The following corollary shows that for separable RLPPs, the effective RLPP is also separable and aggregates uncertainty within and between models.

**Corollary 1.** *Let each RLPP in the uncertainty class be parameterized by  $\rho$  with prior density  $f(\rho|\theta)$ , let  $\Phi$  be an independent labeling process with a probability mass  $P(\Phi = \phi)$  that depends on neither  $\theta$  nor  $\rho$ , and denote the conditional distribution of points by  $f(\mathbf{x}|y, \rho, \theta)$ . Then the effective RLPP is separable*

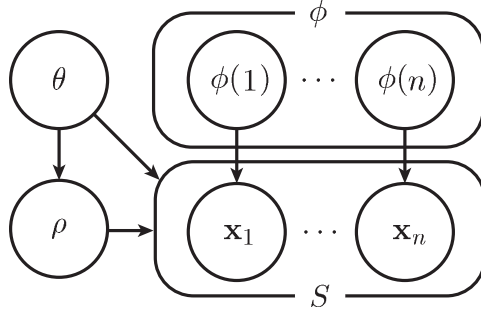


Fig. 1. A graphical model of the uncertainty class of RLPPs assumed in Corollary 1. The parameter  $\theta$  is governed by a prior distribution  $\pi(\theta)$  and indexes each RLPP in the uncertainty class. The number of points,  $n$ , may be generated from an independent process, or considered fixed. For fixed  $n$ , the label function,  $\phi$ , is generated according to the probability mass function  $P(\Phi = \phi)$ . Given  $\theta$ ,  $\rho$  is generated from the density  $f(\rho|\theta)$ , and each point in the point set  $S = \{\mathbf{x}_1, \dots, \mathbf{x}_n\}$  is drawn from the density  $f(\mathbf{x}|y, \rho, \theta)$ , where the corresponding label for point  $\mathbf{x}_i$  is  $y = \phi(i)$ .

with parameter  $[\theta, \rho]$ , prior  $f(\theta, \rho)$ , an independent labeling process with probability mass  $P(\Phi = \phi)$ , and conditional distributions  $f(\mathbf{x}|y, \rho, \theta)$ .

*Proof.* Let the number of points,  $n$ , and the label function  $\phi : \{1, \dots, n\} \rightarrow L^n$  be fixed. For a fixed  $\theta$ , the effective random point process  $\Xi_{\text{eff}}(\omega)$  is set equal to  $\Xi_{\theta}(\omega)$ . Equivalently, a realization of  $S = \{\mathbf{x}_1, \dots, \mathbf{x}_n\}$  under the effective RLPP is governed by the distribution

$$f(S|\phi) = \int \left( \int \left( \prod_{i=1}^n f(\mathbf{x}_i|\phi(i), \rho, \theta) \right) f(\rho|\theta) d\rho \right) \pi(\theta) d\theta.$$

This is equivalent to a separable random point process with parameter  $[\theta, \rho]$ , prior  $f(\theta, \rho) = \pi(\theta)f(\rho|\theta)$  and conditional distributions  $f(\mathbf{x}|y, \rho, \theta)$ . Since the labeling process is independent, the full effective RLPP is the separable RLPP given in the statement of the corollary.  $\square$

A graphical model of the uncertainty class of RLPPs assumed in Corollary 1 is provided in Fig. 1. The IBR clusterer can be found as follows.

- 1) We input an uncertainty class of RLPPs of the form stated in Corollary 1 and illustrated in Fig. 1. In particular, we require the sample size,  $n$ , prior  $\pi(\theta)$ , label process probability mass function  $P(\Phi = \phi)$ , parameter prior  $f(\rho|\theta)$  and conditional density  $f(\mathbf{x}|y, \rho, \theta)$ .
- 2) By Corollary 1, the effective RLPP is found by merging uncertainty in the state (across RLPPs) and parameters (within RLPPs). In particular, the effective RLPP is characterized by the sample size  $n$ , label process probability mass function  $P(\Phi = \phi)$ , parameter prior  $f(\theta, \rho)$  and density  $f(\mathbf{x}|y, \rho, \theta)$ .
- 3) By Theorem 1, the IBR clusterer is the Bayes (optimal) clusterer under the effective RLPP. Given point set  $S$ , the IBR clusterer outputs the partition  $\mathcal{P}_S$  corresponding to the minimal error  $\varepsilon(S, \mathcal{P}_S)$  in (11). The natural cost function  $c_S$  is a constant function given by (10), the partition probabilities are given by (9), and the label function probabilities  $P(\Phi_S = \phi_S|S)$  under the effective (separable) RLPP are given by (12) and the likelihood function (13) with  $f(\theta, \rho)$  in place of  $f(\rho)$  and  $f(\mathbf{x}|y, \rho, \theta)$  in place of  $f(\mathbf{x}|y, \rho)$ .

In practice, the primary issues are: (a) deriving an analytical form for the label function probability,  $P(\Phi_S = \phi_S|S)$ , (b) evaluating the natural cost,  $c_S$ , for all pairs of partitions, and (c) evaluating partition errors,  $\varepsilon(S, \mathcal{P}_S)$ , for all partitions. Note that  $P(\Phi_S = \phi_S|S)$  is available for Gaussian separable RLPPs in (16). Issues (b) and (c) may also be alleviated using optimal and suboptimal algorithms, as discussed in [1].

#### IV. ROBUST CLUSTERING UNDER GAUSSIAN RLPPS

Consider synthetic Gaussian data with  $l = 2$  clusters in  $d = 1, 2, 10, 100$  and  $1,000$  dimensions. The state of nature is composed of the cluster covariances, and for a given state of nature the point

process generates equal sized Gaussian clusters with random means and the corresponding covariances. Formally, we parameterize the uncertainty class of RLPPs with  $\theta = [\theta_1, \theta_2]$ , where  $\theta_y = \Sigma_y$ , and each  $\Sigma_y$  is drawn independently from an inverse-Wishart distribution with  $\kappa_y$  degrees of freedom and scale matrix  $\Psi_y$ . The RLPP in the uncertainty class corresponding to  $\theta$ ,  $(\Xi_\theta, \Lambda_\theta)$ , is a separable RLPP with parameter  $\rho_y = \mu_y$ , Gaussian prior  $f(\rho_y)$  with mean  $\mathbf{m}_y$  and covariance  $\Sigma_y/\nu_y$ , and Gaussian conditional distributions  $f(\mathbf{x}|y, \rho_y, \theta_y)$  with mean  $\mu_y$  and covariance  $\Sigma_y$ . We set  $\kappa_1 = \kappa_2 = d+2$ ,  $\Psi_1 = \Psi_2$  to be  $d \times d$  identity matrices,  $\nu_1 = \nu_2 = 1$ , and  $\mathbf{m}_1 = \mathbf{m}_2$  to be all-zero vectors. The number of points,  $n = n_1 + n_2$ , is set to 10 or 100 with  $n_1 = n_2$ , and the labels are permuted. Thus, the true distribution on label functions,  $P(\Phi = \phi)$ , has a support on the set of label functions that assign the correct number of points to each cluster, and is uniform on its support.

For each combination of  $d$  and  $n$ , we generate 1,000 states of nature,  $\theta$ , and one point set per state of nature from the corresponding separable RLPP  $(\Xi_\theta, \Lambda_\theta)$ . For each point set, we run several classical clustering algorithms: fuzzy  $c$ -means (FCM),  $k$ -means (KM), hierarchical clustering with single linkage (H-S), hierarchical clustering with average linkage (H-A), hierarchical clustering with complete linkage (H-C), and a clusterer that produces a random partition with equal sized clusters for reference (Random). More details about these algorithms may be found in [19]. In addition, we cluster using expectation maximization for Gaussian mixture models (EM), and a method that minimizes a lower bound on the posterior expected variation of information under an estimated posterior similarity matrix generated from samples of a Gibbs sampler for Gaussian mixture models (MCMC) [20]. EM is run using the `mclust` package in R with default settings [21], [22], [23]. The Gibbs sampler is implemented using the `bayesm` package in R with 18,000 samples generated after a burn-in period of 2,000 samples, and otherwise default settings [24]. The posterior similarity matrix is estimated using the `mclust` package in R [25], and minimization with respect to variation of information is implemented with the `mclust.ext` package in R [26]. We also implement EM informed with the ‘‘correct’’ hyperparameters,  $\kappa_y$ ,  $\Psi_y$ ,  $\nu_y$  and  $\mathbf{m}_y$  (EM-I) and MCMC informed with the ‘‘correct’’ hyperparameters (MCMC-I).

To find the IBR clusterer, the effective RLPP,  $(\Xi, \Lambda)$ , is constructed using Corollary 1, which states that the effective RLPP merges uncertainty in the state  $\theta$  with uncertainty in the parameter  $\rho$ . In this case, the effective RLPP is precisely the separable RLPP presented in Section II-B, which accounts for both random means in  $\rho$  and random covariances in  $\theta$ . The effective RLPP is solvable (at least for small point sets) using the Bayes clusterer presented in [1]. By Theorem 1, the IBR clusterer is equivalent to the Bayes clusterer under the effective RLPP. Thus, the IBR clusterer can be found when  $n = 10$  by evaluating (8) for all partitions using (9) and (18), and choosing the minimizing partition. When  $n = 100$ , we approximate the IBR clusterer (IBR-A) using a sub-optimal algorithm, Suboptimal Pseed Fast, presented in [1], which finds the maximum probability partition for a random subset of 10 points, generalizes these clusters to the full point set using a QDA classifier, iteratively searches for the highest probability partition on the full point set by considering all partitions with at most two points clustered differently from the best partition found so far, and finally chooses the highest probability partition resulting from 10 repetitions with different initial subsets of points. MCBR and minimax robust clusterers are not found, since they are computationally infeasible. Furthermore, having found an IBR clusterer one would certainly not use an MCBR clusterer and very likely not use a minimax robust clusterer.

For each point set and each algorithm, we find the cluster mismatch error between the true partition and the algorithm output using (6). For each combination of  $d$  and  $n$  and each algorithm, we approximate the average partition error,  $E_\theta[\varepsilon_\theta(\zeta)]$ , under the natural cost function using the average cluster mismatch error across all 1,000 point sets. Figure 2(a) presents a graph of these errors with respect to  $d$  for  $n = 10$ , and similarly Figure 2(b) presents performance for  $n = 100$ . These graphs support the fact that the IBR clusterer is optimal in these simulations when  $n = 10$ , and that the approximate IBR clusterer is close to optimal when  $n = 100$ . Indeed, the IBR clusterer performs significantly better than all other algorithms under high dimensions.

When the number of points is large ( $n = 100$ ) and the number of dimensions ( $d$ ) is smaller than the number of points, the performances of EM and EM-I are very close to the approximate IBR clusterer. However,

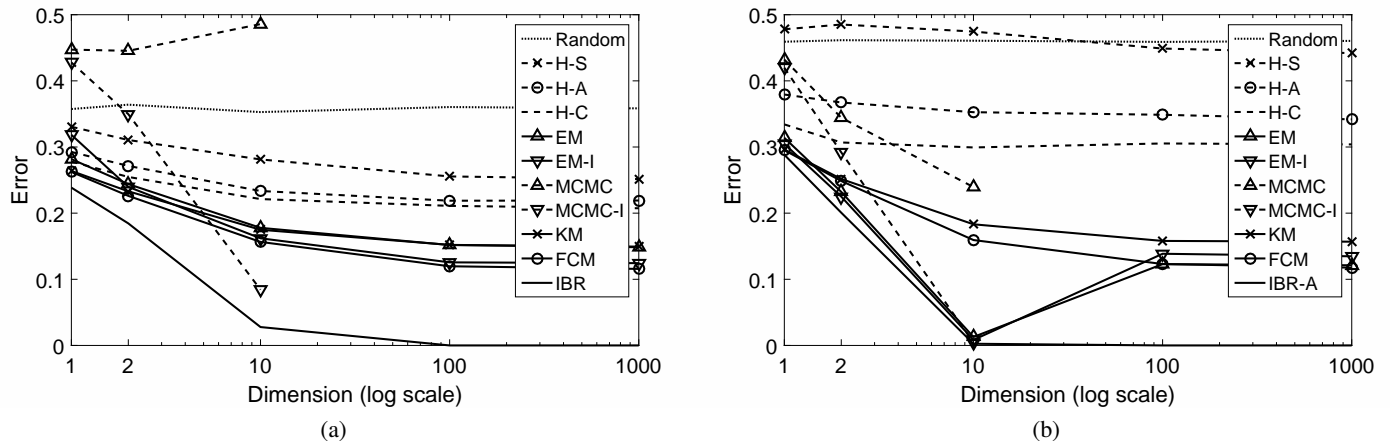


Fig. 2. Average cluster mismatch error for Gaussian RLPPs: (a)  $n = 10$ , (b)  $n = 100$ .

when the number of points is small, or the number of dimensions is larger than the number of points, these algorithms tend to be similar to FCM and KM. This is most likely because mclust tests several different modeling assumptions regarding the covariances, and uses the Bayesian information criterion (BIC) to select a final output partition. When  $n$  is small relative to  $d$ , the full covariances of the Gaussian mixtures cannot be estimated well, so there is a tendency to select simpler models that assume covariances are equal and circular, which is essentially the same assumption made by FCM and KM. Finally note that MCMC by default uses a particular normal-inverse-Wishart prior with hyperparameters that do not match the “correct” hyperparameters. The fact that MCMC-I performs much better than MCMC suggests that this method may be quite sensitive to the priors, especially when the sample size is small.

## V. ROBUST CLUSTERING IN GRANULAR IMAGING

While digital photography may now dominate over chemical photography, silver-based imaging remains important and is currently growing in use. Research remains active. Crystal shape is of particular importance. For many years granulometric analysis has been important in particle and texture analysis. In particular, morphological granulometries can generate image features relating to the size, shape, and concentration of particles. We present an application of robust clustering for images of silver-halide photographic T-grain crystals with respect to grain proportions using granulometric features.

### A. Morphological Granulometries

A basic model for silver-halide emulsions includes grains that are equilateral triangles, hexagons formed by removing triangle corners, rods (rectangles), and ill-formed blobs. To simplify calculations, we focus on a binary image model using only triangles and rods. In film grade emulsions grains overlap, but for laboratory analysis diluted emulsions with negligible overlapping can be produced, thus we also focus on images with non-overlapping grains.

Morphological granulometries are particularly well-suited for modeling and processing binary images consisting of grains of different sizes and shapes. The most commonly employed granulometry is a family of parameterized morphological openings: for a convex, compact *structuring element* (set)  $B$ , a *granulometry*  $\{\Psi_t\}$  is defined by  $\Psi_t(I) = I \circ tB$  for  $t > 0$  and  $\Psi_0(I) = I$ , where  $I \circ tB = \cup\{tB + x : tB + x \subset I\}$  is the opening of image (set)  $I$  by  $tB$  (more general granulometries exist [12]). If  $\Omega_I(t)$  is the area of  $\Psi_t(I)$ , then  $\Omega_I(t)$  is a decreasing function of  $t$ , known as a *size distribution*. A normalized size distribution is defined by  $\Phi_I(t) = 1 - \Omega_I(t)/\Omega_I(0)$ . If  $I$  is compact and  $B$  consists of more than a single point, then  $\Phi_I(t)$  increases from 0 to 1 and is continuous from the left. Thus, it defines a probability distribution function called the *pattern spectrum* of  $I$  (relative to  $B$ ). Moments of  $\Phi_I(t)$  are used for

image classification and segmentation [27].  $\Phi_I(t)$  is a random function and its non-central moments (called *granulometric moments*) are random variables.

In this work, we use granulometric moments as features for clustering. Given a set  $I$ , we extract as features the first  $q$  granulometric moments of  $I$  generated by granulometries arising from  $p$  structuring elements  $B_1, B_2, \dots, B_p$ , where we denote the  $k$ th granulometric moment corresponding to  $B_j$  by  $\mu^{(k)}(I, B_j)$  for  $j = 1, 2, \dots, p$  and  $k = 1, 2, \dots, q$ . Consider a random set  $I$  of the form

$$I = \bigcup_{i=1}^m \bigcup_{j=1}^{N_i} (r_{ij}A_i + x_{ij}), \quad (23)$$

where  $A_1, A_2, \dots, A_m$  are compact sets called *primitives*,  $r_{ij}$  and  $x_{ij}$  specify the radius (grain size) and center of the  $j$ th grain of primitive type  $i$ , respectively, and all  $N = N_1 + \dots + N_m$  grains are mutually disjoint.

In the silver halide application, we assume preprocessed images are well modeled by (23), where  $m = 2$ ,  $A_1$  is an equilateral triangle with horizontal base, and  $A_2$  is a vertical rod with height 5 times its base. Without loss of generality, we assume both primitives have unit area, i.e.,  $\nu[A_1] = \nu[A_2] = 1$ , and we denote the grain proportions by  $b_1$  and  $b_2$ . We further assume the  $r_{ij}$  are independent with the  $r_{i1}, \dots, r_{iN_i}$  identically distributed, where the *grain sizing distribution* for primitive  $i$  has the property  $E[r_{ij}^k] = \gamma_{ik}\beta^k$  for all  $k > 0$  and  $\gamma_{ik}$  and  $\beta$  are positive constants. If  $r_{ij} \sim \text{gamma}(\alpha_i, \beta)$ ,  $\beta$  being the scale parameter for both primitives, then this property holds with  $\gamma_{ik} = \Gamma(\alpha_i + k)/\Gamma(\alpha_i)$ .

For the morphological opening, we use  $p = 2$  structuring elements, where  $B_1$  and  $B_2$  are, respectively, vertical and horizontal linear structuring elements. The first  $q = 2$  granulometric moments for  $B_1$  and  $B_2$  are

$$\mathbf{z} = [\mu^{(1)}(I, B_1) \ \mu^{(1)}(I, B_2) \ \mu^{(2)}(I, B_1) \ \mu^{(2)}(I, B_2)]^T.$$

Given the constants  $\mu^{(k)}(A_i, B_j)$  and the radii  $r_{ij}$  of all grains, the exact moments in  $\mathbf{z}$  under the granulometric model may be found analytically (see Theorem 3 in the Appendix). In particular,  $\mathbf{z} = M\mathbf{x}$ , where

$$M = \begin{bmatrix} \mu^{(1)}(A_1, B_1) & \mu^{(1)}(A_2, B_1) & 0 & 0 \\ \mu^{(1)}(A_1, B_2) & \mu^{(1)}(A_2, B_2) & 0 & 0 \\ 0 & 0 & \mu^{(2)}(A_1, B_1) & \mu^{(2)}(A_2, B_1) \\ 0 & 0 & \mu^{(2)}(A_1, B_2) & \mu^{(2)}(A_2, B_2) \end{bmatrix},$$

and  $\mathbf{x} = [x_{11}, x_{21}, x_{12}, x_{22}]^T$ , where

$$x_{ik} = \frac{\sum_{j=1}^{N_i} r_{ij}^{k+2}}{\sum_{j=1}^{N_1} r_{1j}^2 + \sum_{j=1}^{N_2} r_{2j}^2}. \quad (24)$$

In general, the constants  $\mu^{(k)}(A_i, B_j)$  under convex grains can be found using theory from [28]. It can be shown that for triangle  $A_1$  and vertical structuring element  $B_1$  that  $\mu^{(1)}(A_1, B_1) = 2 \cdot 3^{-3/4}$  and  $\mu^{(2)}(A_1, B_1) = 2^{-1}3^{1/2}$ . Similarly, for other combinations of primitives and structuring elements,  $\mu^{(1)}(A_1, B_2) = 4 \cdot 3^{-5/4}$ ,  $\mu^{(2)}(A_1, B_2) = 2 \cdot 3^{-1/2}$ ,  $\mu^{(1)}(A_2, B_1) = 5^{1/2}$ ,  $\mu^{(2)}(A_2, B_1) = 5$ ,  $\mu^{(1)}(A_2, B_2) = 5^{-1/2}$  and  $\mu^{(2)}(A_2, B_2) = 5^{-1}$ .

In the current application, we cluster on the features  $\mathbf{x} = M^{-1}\mathbf{z}$ . Lemma 1 in the Appendix guarantees asymptotic joint normality and provides analytic expressions for the asymptotic mean and covariance of granulometric moments under multiple primitives and multiple structuring elements. In particular, given the grain proportions  $b_1$  and  $b_2$ , and the grain sizing parameters  $\beta$  and  $\gamma_{ik}$  for  $i = 1, 2$  and  $k = 2, 3, 4$ ,  $\mathbf{x}$  has asymptotic mean

$$\frac{1}{b_1\gamma_{12} + b_2\gamma_{22}} [b_1\gamma_{13}\beta \quad b_2\gamma_{23}\beta \quad b_1\gamma_{14}\beta^2 \quad b_2\gamma_{24}\beta^2]^T \quad (25)$$

and covariance matrix

$$\frac{1}{N(b_1\gamma_{12} + b_2\gamma_{22})^4} \begin{bmatrix} A_{11}\beta^2 & A_{12}\beta^3 \\ A_{21}\beta^3 & A_{22}\beta^4 \end{bmatrix}, \quad (26)$$

where the  $A_{ij}$  are  $2 \times 2$  matrices that depend on only the  $b_i$  and  $\gamma_{ik}$ , and are provided in the Appendix.

### B. Robust Clustering

Suppose we are given a collection of  $n$  binary images of mixtures of silver-halide photographic T-grain crystals, where each image belongs to one of two groups, indexed by  $y = 1, 2$ . Images in class 1 and 2 have different proportions of triangles,  $b_1$ , and different sizing parameters, thereby providing different photographic properties. Our objective is to cluster the images into the two groups (our concern is partitioning, not labeling) based on feature vectors  $\mathbf{x} = M^{-1}\mathbf{z}$  obtained from moments of morphological openings  $\mathbf{z}$ .

Given the grain sizing distributions and a prior  $f(\rho)$ , the asymptotic joint normality of  $\mathbf{x}$  motivates a separable RLPP model where, given  $y$  and  $\rho$ ,  $f(\mathbf{x}|y, \rho)$  is a Gaussian distribution with mean and covariance given by (25) and (26), respectively. We substitute  $\rho$  and  $1 - \rho$  in place of  $b_1$  and  $b_2$  under class 1, and vice-versa under class 2. For simplicity, we assume  $P(\Phi = \phi)$  is uniform with support such that the number of images in each class is known.

The grain sizing distribution in a binarized image typically depends on the image thresholding method and other factors, and thus is unknown. To account for this, we model an uncertainty class of RLPPs parameterized by  $\theta$ , where the grain sizes are assumed to be gamma( $\alpha_{iy}, \beta_y$ ) distributed, the  $\alpha_{iy}$  parameters are fixed and known, the  $\beta_y$  depend deterministically on  $\theta$ , and we assume  $\theta$  and  $\rho$  are mutually independent with known prior  $\pi(\theta)$ . From (12) and (13), the IBR clusterer reduces to finding the following label function probabilities under the effective RLPP:

$$P(\Phi_S = \phi_S|S) \propto P(\Phi = \phi) \times \int_0^\infty \int_0^1 f(S_1|1, \rho, \theta) f(S_2|2, \rho, \theta) f(\rho) \pi(\theta) d\rho d\theta, \quad (27)$$

where

$$f(S_y|y, \rho, \theta) = \prod_{\mathbf{x} \in S_y} f(\mathbf{x}|y, \rho, \theta).$$

Since we assume a Gaussian model,  $f(S_y|y, \rho, \theta)$  is precisely the likelihood function in (15). To make (27) tractable, we assume discrete priors on  $\rho$  and  $\theta$  so that the integrals can be written as sums.

### C. Experimental Results

The image generation model is based on the parameterized RLPP model described above. For a given set of images under a given RLPP with parameter  $\theta$ , which determines the sizing distribution, we generate  $n = n_1 + n_2$  binary images, where  $n_1$  and  $n_2$  denote the fixed number of images from class 1 and class 2, respectively. Each image contains 1,000 non-overlapping and vertically aligned grains (triangles and rods), and is  $550 \times 550$  pixels. The prior  $f(\rho)$  on the proportion of triangles for class 1 is uniform over 500 values from 0.45 to 0.55, and we assume the proportion of triangles for class 2 is  $1 - \rho$ . Figure 3 shows three example realizations of images with gamma( $\alpha = 1.95, \beta = 2$ ) sizing distributions for the triangles and gamma( $\alpha = 1.97, \beta = 2$ ) for the rods. Parts (a), (b), and (c) contain triangle proportions 0.45, 0.5, and 0.55, respectively.

The prior  $\pi(\theta)$  is uniform over 10 values from 1.75 to 2. We assume gamma( $\alpha_{iy}, \beta_y$ ) sizing distributions for primitive  $i$  under class  $y$ , where  $\beta_1 = \theta$ ,  $\beta_2 = 3.75 - \theta$ . For triangles,  $\alpha_{1y} = 1.95$  and  $1.97$  for class 1 and class 2, respectively, and for rods,  $\alpha_{2y} = 1.97$  and  $1.95$  for class 1 and class 2, respectively. We generate 500 sets of images for each state, for a total of 5,000 sets of images. For each image, openings are found, followed by granulometric moments  $\mathbf{z}$  from the openings, and finally a feature vector  $\mathbf{x} = M^{-1}\mathbf{z}$ .

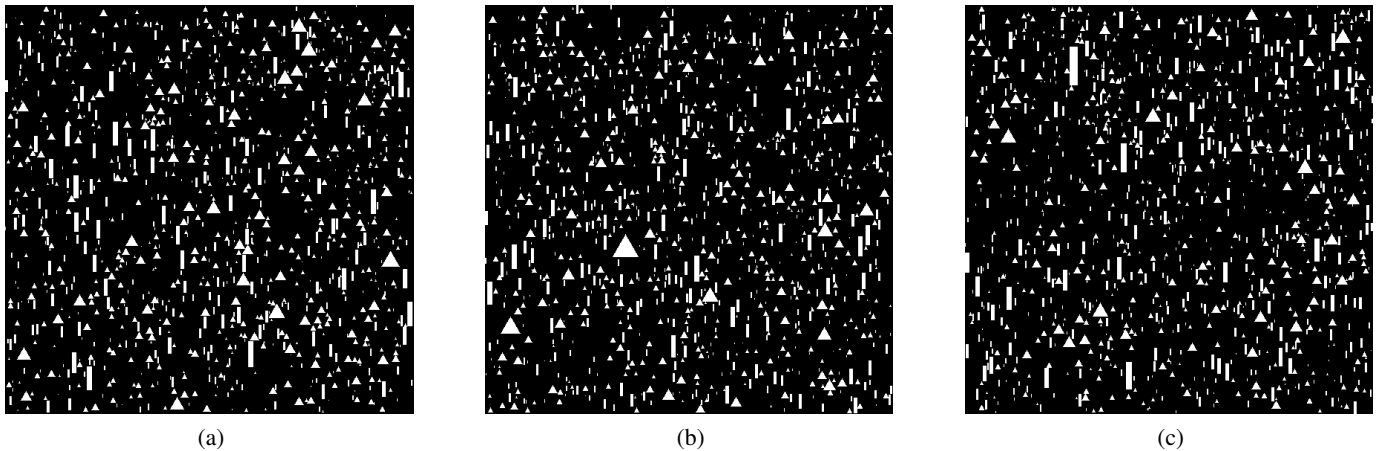


Fig. 3. Examples of image realizations generated by the T-grain crystal model. Each image contains 1,000 grains. The sizing distribution of the grains are gamma( $\alpha = 1.95, \beta = 2$ ) for the triangles and gamma( $\alpha = 1.97, \beta = 2$ ) for the rods. The size of each image is  $550 \times 550$  pixels: (a) proportions of 0.45 triangles and 0.55 rods, (b) 0.5 triangles and 0.5 rods, and (c) 0.55 triangles and 0.45 rods.

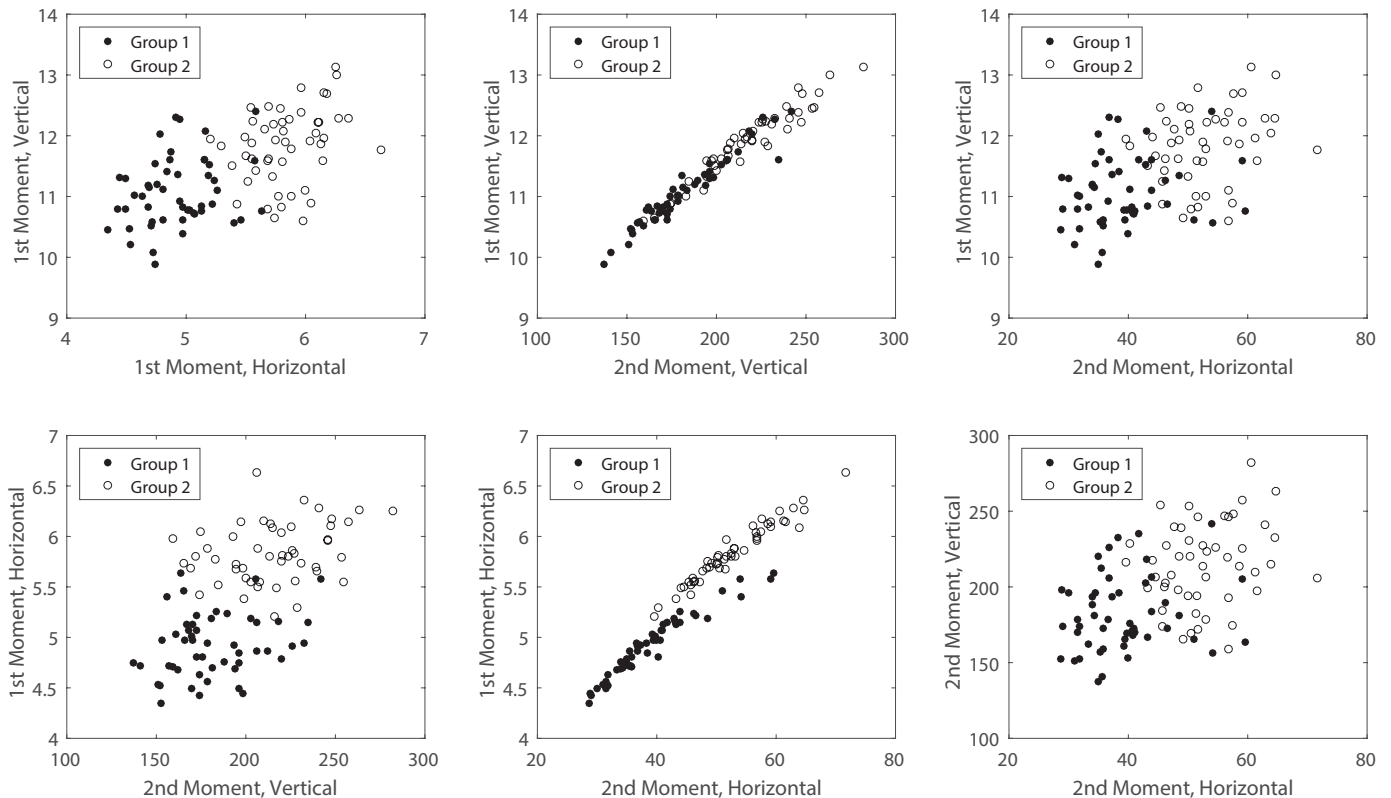


Fig. 4. Scatter plots of all pairs of features extracted from 100 images.

Figure 4 provides example scatter plots of all pairs of features extracted from 100 images. These images correspond to  $\theta = 1.75$  and the 10 smallest values of  $\rho$  (between 0.45 and 0.452), with 5 images selected from each value of  $\rho$  and each group.

For each set of images, we run FCM, KM, H-S, H-A, H-C, EM, MCMC and Random. Note EM-I and MCMC-I, which use normal-inverse-Wishart priors on the mean and covariance pairs, are not sensible to run here since the model uncertainty on  $b_1$ ,  $b_2$  and  $\beta$  is not very compatible with this prior form. We also find the IBR partition using the Bayes partition for the effective RLPP, which merges uncertainty in  $\theta$  and  $\rho$ . In particular, we compute the partition error for all partitions of the images from (11), and choose

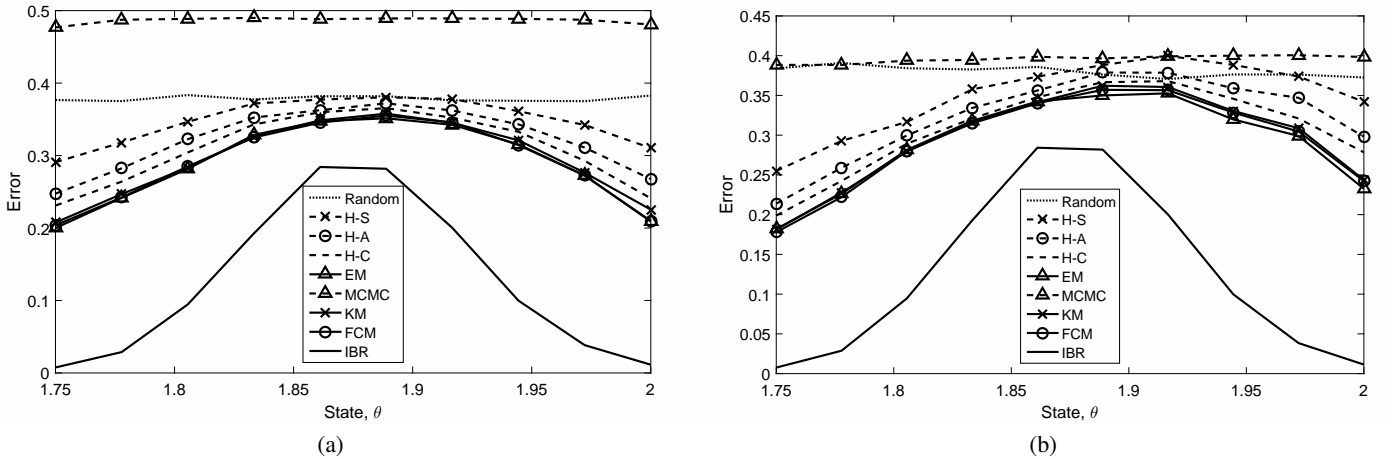


Fig. 5. Average cluster mismatch error as a function of the state,  $\theta$ , in the granular imaging example: (a)  $n_1 = n_2 = 5$ , (b)  $n_1 = 6$  and  $n_2 = 4$ .

TABLE I  
AVERAGE CLUSTER MISMATCH ERROR OVER ALL 5,000 ITERATIONS IN THE GRANULAR IMAGING EXAMPLE.

$n_1, n_2$	IBR	FCM	KM	MCMC	EM	H-C	H-A	H-S	Random
5, 5	0.1239	0.2899	0.2938	0.4858	0.2890	0.3086	0.3223	0.3477	0.3786
6, 4	0.1351	0.2924	0.2952	0.3956	0.2904	0.3079	0.3224	0.3488	0.3799

the partition with minimal partition error. Note that (11) is found using the natural cost function in (10), and the posterior partition probabilities in (9), which is based on posterior label function probabilities that may be computed exactly using a discretized version of (27). Recall  $f(\mathbf{x}|y, \rho, \theta)$  is assumed Gaussian with means given by (25), covariances given by (26), and appropriate values for  $b_1$ ,  $b_2$  and  $\beta$  depending on  $y$ ,  $\rho$  and  $\theta$ . It is possible to list all partitions and compute the partition errors exactly when  $n = 10$  and  $l = 2$ . Again, we did not test MCBR and minimax robust clusters owing to their high computational cost.

Figure 5 shows the approximate clustering error for all algorithms with respect to  $\theta$ , computed using the average cluster mismatch error over 500 sets of images for each  $\theta$ . Part (a) shows results when  $n_1 = n_2 = 5$ , and part (b) shows results when  $n_1 = 6$  and  $n_2 = 4$ . In both parts (a) and (b), the IBR clusterer performs much better than all classical algorithms across all states. Note that the IBR clusterer makes “incorrect” Gaussian modeling assumptions, but that the Gaussianity assumption and the analytically computed mean and covariance for each cluster become more accurate as the number of grains increases. Under all algorithms there is a significant variation in performance, which deteriorates when  $\theta \approx 1.8750$ . This corresponds to the case where  $\beta_1 = \beta_2$ , i.e., the case where the classes are most similar. Among all classical algorithms, the EM algorithm is usually the best, followed by FCM and KM, which have very similar performance. In some cases in Figure 5, the performance of hierarchical clustering with single linkage is worse than Random. As seen in Section IV, MCMC with incorrect priors and small samples again has very poor performance. These graphs are summarized in Table I, which shows the approximate average clustering error for each algorithm over all states and iterations. Finally, note that performance is similar between equal and unequal cluster size for all algorithms.

Since our focus is on robust clustering theory rather than image processing, in particular, the interplay between clustering optimization and the structure of prior knowledge, we have implemented a model setting based on (23); nevertheless, before concluding this section, we believe a few comments concerning the effect of deviations from the model assumptions on the asymptotic granulometric moments are warranted.

The grain model of (23) has been used in numerous studies of granulometric filtering and asymptotic moment analysis. Three issues regarding robustness of the theory to deviations from model assumptions

have been addressed in [29]: (1) assuming a certain sizing distribution when in fact the random set satisfies a different sizing distribution, (2) using erroneous parameters for the sizing distribution, and (3) prior segmentation when there is modest overlapping.

For instance, the effect of erroneous  $\gamma(\alpha, \beta)$  sizing was analytically quantified with respect to misclassification error. Perhaps more importantly, the effect of watershed segmentation to separate overlapping grains prior to moment analysis was quantified by establishing lower and upper bounds on the actual  $k$ th granulometric moments when there are multiple grain primitives. One could reconsider the entire clustering analysis relative to these bounds; however, given the complexity of the bounds, this would involve a complicated mathematical study that would lead us far afield. The bounds are quite tight when grain overlapping is minor, as it is with a properly prepared emulsion.

Finally, as in all asymptotic granulometric theory, grain orientation is assumed fixed and not subject to rotation. The assumption is that each grain can be canonically rotated so that triangles have a horizontal base and for rods the shorter side forms the base, as assumed in the model. Robustness relative to imperfect rotation normalization has not been studied analytically. In fact, in digital image processing, rotation can cause problems for triangles and rectangles when edge detection is inaccurate, which is troublesome when there is low pixel resolution, a situation that is much less problematic today than when the basic granulometric theory was developed twenty years ago.

## VI. CONCLUSION

We have extended the theories of robust filtering and classification to clustering and developed new theory showing that optimal Bayesian robust clustering can be viewed as two equivalent optimization problems, one based on a parameterized uncertainty class of RLPPs and the other on a single effective RLPP that absorbs all parameters in the model. Thus, one can first focus on modeling the uncertainties and then focus on finding the Bayes clusterer (or a good approximation) for the effective model.

The proposed paradigm for robust clustering is distinct from all other clustering methods in that it is fully model-based, can account for all prior knowledge and sources of uncertainty, and is optimal relative to clustering error. A key part of the paradigm involves justifying the modeling assumptions. In cases where the modeling assumptions can be justified, like in our granular imaging example where we developed new theory on the asymptotic joint normality and moments of our extracted features, we now have a very powerful theory for optimal robust clustering. Furthermore, since the Bayes and IBR clusterers employ powerful optimization directly with respect to clustering error (or clustering risk if used with specialized cost functions), under small to moderate imperfections of the assumed model they often continue to outperform many principled optimization-based methods. For instance, although our implementations of the EM, MCMC and IBR algorithms all assume Gaussian mixture models, EM and MCMC do not always perform as well as IBR because: (1) they focus on estimating the means and covariances instead of minimizing error, (2) they are often implemented without available prior knowledge.

We conclude with a note on computational complexity. The optimal IBR clusterer under Gaussian models is computationally expensive, which remains an important issue. Since our objective here has been to develop a theory of robust clustering, we have focused on clustering a small number of points and implemented optimal algorithms whenever possible. That being said, suboptimal methods inspired by the optimal equations for the Bayes clusterer under Gaussian models (e.g., Suboptimal Pseed Fast) have been presented in [1]. These have nearly optimal performance and competitive computation time with point sets of size up to 10,000. We aim to continue studying fast suboptimal algorithms for the Bayes clusterer in future work, which by Theorems 1 and 2 automatically extend to algorithms for robust clustering.

## APPENDIX

Here, we justify modeling assumptions like normality used by the IBR clusterer in the granular imaging example. The following theorems, originally proved in [30] and [31], provide exact expressions for granulometric moments as a function of the grain radii. They state that any finite length vector of

granulometric moments from a single structuring element is asymptotically normal, and provide analytic expressions for the asymptotic mean and variance of moments. The covariance of moments is available in [31].

**Theorem 3.** *Let  $I$  be modeled as in (23). For the granulometry  $\{I \circ tB\}$  generated by a convex, compact structuring element  $B$ , and for  $k \geq 1$ ,*

$$\mu^{(k)}(I, B) = \frac{u}{v} \equiv H(u, v), \quad (28)$$

where

$$u = \frac{1}{N} \sum_{i=1}^m \sum_{j=1}^{N_i} \mu^{(k)}(A_i, B) \nu[A_i] r_{ij}^{k+2}, \quad (29)$$

$$v = \frac{1}{N} \sum_{i=1}^m \sum_{j=1}^{N_i} \nu[A_i] r_{ij}^2, \quad (30)$$

$\nu[A_i]$  is the volume of  $A_i$ , and  $\mu^{(k)}(A_i, B)$  is the  $k$ th moment of  $A_i$  under structuring element  $B$ . Moreover, suppose:

- 1) The proportions  $b_i = N_i/N$  are known and fixed.
- 2) The  $r_{ij}$  are independent,  $r_{i1}, \dots, r_{iN_i}$  are identically distributed, and every  $r_{ij}$  has finite moments up to at least order  $k + 2$ .
- 3) There exist  $c$  and  $t > 0$  such that  $H \leq cN^t$  for  $N > 1$ .
- 4)  $H$  has first and second derivatives, with bounded second derivatives in a neighborhood of  $(E[u], E[v])$ .

Then the distribution of  $H$  is asymptotically normal as  $N \rightarrow \infty$  with mean and variance given by

$$E[H] = H(E[u], E[v]) + O(N^{-1}) \quad (31)$$

and

$$\begin{aligned} \text{Var}[H] &= \left(\frac{\partial H}{\partial u}(E[u], E[v])\right)^2 \text{Var}[u] \\ &+ 2 \frac{\partial H}{\partial u}(E[u], E[v]) \frac{\partial H}{\partial v}(E[u], E[v]) \text{Cov}[u, v] \\ &+ \left(\frac{\partial H}{\partial v}(E[u], E[v])\right)^2 \text{Var}[v] + O(N^{-3/2}). \end{aligned} \quad (32)$$

**Theorem 4.** *Under the conditions of Theorem 3, any finite set of granulometric moments is asymptotically jointly normal.*

Theorems 3 and 4 are not sufficient to guarantee the asymptotic joint normality of  $\mathbf{x}$  or  $\mathbf{z}$ , or to obtain their asymptotic moments, because these vectors contain moments from multiple structuring elements. Thus, here we present a new lemma proving asymptotic joint normality and providing analytic expressions for the asymptotic mean and covariance of granulometric moments under multiple primitives and multiple structuring elements. It can be shown that these moments are consistent with (31) and (32).

**Lemma 1.** *Let  $I$  be modeled as in (23) with  $m = 2$  primitives, let  $b_1 = N_1/N$  and  $b_2 = N_2/N$  be known and fixed, and let the radii  $r_{ij}$  be independent such that  $r_{i1}, \dots, r_{iN_i}$  are identically distributed and  $E[r_{ij}^k] = \gamma_{ik} \beta^k$  for  $k = 2, 3, 4$ . Let  $\mathbf{x} = M^{-1} \mathbf{z}$  be a vector of linearly transformed first and second order granulometric moments under arbitrary structuring elements,  $B_1$  and  $B_2$ . Then  $\mathbf{x}$  is asymptotically jointly normal with mean vector*

$$\frac{1}{b_1 \gamma_{12} + b_2 \gamma_{22}} [b_1 \gamma_{13} \beta \quad b_2 \gamma_{23} \beta \quad b_1 \gamma_{14} \beta^2 \quad b_2 \gamma_{24} \beta^2]^T \quad (33)$$

and covariance matrix

$$\frac{1}{N(b_1\gamma_{12} + b_2\gamma_{22})^4} \begin{bmatrix} A_{11}\beta^2 & A_{12}\beta^3 \\ A_{21}\beta^3 & A_{22}\beta^4 \end{bmatrix}, \quad (34)$$

where

$$\begin{aligned} A_{ij} &= \begin{bmatrix} (b_1)^2(b_1B_{ij1}^{11} + b_2B_{ij1}^{12}) & b_1b_2(b_1B_{ij1}^{21} + b_2B_{ij1}^{22}) \\ b_1b_2(b_1B_{ij2}^{11} + b_2B_{ij2}^{12}) & (b_2)^2(b_1B_{ij2}^{21} + b_2B_{ij2}^{22}) \end{bmatrix} \\ &\quad + \begin{bmatrix} b_1(b_1\gamma_{12} + b_2\gamma_{22})^2C_{ij1} & 0 \\ 0 & b_2(b_1\gamma_{12} + b_2\gamma_{22})^2C_{ij2} \end{bmatrix}, \\ B_{ijk}^{lp} &= C_{00p}\gamma_{k(i+2)}\gamma_{l(j+2)} \\ &\quad - \gamma_{p2}\gamma_{k(i+2)}C_{0jl} - \gamma_{p2}C_{i0k}\gamma_{l(j+2)}, \\ C_{ijk} &= \gamma_{k(i+j+4)} - \gamma_{k(i+2)}\gamma_{k(j+2)}. \end{aligned}$$

*Proof.* Note  $\mathbf{x} = [x_{11} \ x_{21} \ x_{12} \ x_{22}]^T$  has components  $x_{ik}$  given by (24). Without loss of generality, assume each primitive has area  $\nu[A_1] = \nu[A_2] = 1$ . Fix  $i$ , and for each  $j = 1, \dots, N_i$  let  $\mathbf{r}_{ij} = [r_{ij}^2 \ r_{ij}^3 \ r_{ij}^3]^T$ .  $\mathbf{r}_{ij}$  is thus a sequence of independent and identically distributed random vectors, and let us denote the common mean vector by  $\mu_i = [\mu_{i2} \ \mu_{i3} \ \mu_{i4}]^T$  and covariance matrix by  $\Sigma_i$ , which are assumed to exist. Then by the central limit theorem,

$$\sqrt{N_i}(\mathbf{r}_i - \mu_i) \longrightarrow \mathcal{N}(\mathbf{0}, \Sigma_i),$$

where  $\mathbf{r}_i$  is the sample mean of the  $\mathbf{r}_{ij}$  over all  $j$ ,  $\mathcal{N}$  denotes a multivariate Gaussian distribution, and “ $\longrightarrow$ ” denotes convergence in distribution. Since the sets of radii  $\{r_{1j}\}$  and  $\{r_{2j}\}$  are independent,  $\mathbf{r}_1$  and  $\mathbf{r}_2$  are independent. Hence, as long as  $N_1$  and  $N_2$  go to infinity as  $N$  goes to infinity, we have for  $\mathbf{w} = [b_1\mathbf{r}_1^T \ b_2\mathbf{r}_2^T]^T$  and  $\mu = [b_1\mu_1^T \ b_2\mu_2^T]^T$ ,

$$\sqrt{N}(\mathbf{w} - \mu) \longrightarrow \mathcal{N}\left(\mathbf{0}, \begin{bmatrix} b_1\Sigma_1 & \mathbf{0} \\ \mathbf{0} & b_2\Sigma_2 \end{bmatrix}\right).$$

Define  $g : \mathbb{R}^6 \rightarrow \mathbb{R}^4$ , where

$$g(\mathbf{w}) = \frac{1}{w_1 + w_4} [w_2 \ w_5 \ w_3 \ w_6]^T$$

for  $\mathbf{w} = [w_1 \ w_2 \ w_3 \ w_4 \ w_5 \ w_6]^T$ .  $g$  is differentiable whenever  $w_1 + w_4 \neq 0$ , and

$$\frac{\partial g}{\partial \mathbf{w}} = \frac{1}{(w_1 + w_4)^2} \times \begin{bmatrix} -w_2 & w_1 + w_4 & 0 & -w_2 & 0 & 0 \\ -w_5 & 0 & 0 & -w_5 & w_1 + w_4 & 0 \\ -w_3 & 0 & w_1 + w_4 & -w_3 & 0 & 0 \\ -w_6 & 0 & 0 & -w_6 & 0 & w_1 + w_4 \end{bmatrix}.$$

Applying the *Multivariate Delta Method* [32], and noting that  $\mu_{12}$  and  $\mu_{22}$  will not both be zero for any reasonable sizing distribution,

$$\begin{aligned} &\sqrt{N}(g(\mathbf{w}) - g(\mu)) \longrightarrow \\ &\mathcal{N}\left(\mathbf{0}, \left(\frac{\partial g}{\partial \mathbf{w}}(\mu)\right) \begin{bmatrix} b_1\Sigma_1 & \mathbf{0} \\ \mathbf{0} & b_2\Sigma_2 \end{bmatrix} \left(\frac{\partial g}{\partial \mathbf{w}}(\mu)\right)^T\right). \end{aligned}$$

Note that  $\mathbf{x} = g(\mathbf{w})$ , and that

$$\frac{\partial g}{\partial \mathbf{w}}(\mu) = \frac{1}{(b_1\mu_{12} + b_2\mu_{22})^2} \begin{bmatrix} G_{11} & G_{12} \\ G_{21} & G_{22} \end{bmatrix},$$

where

$$\begin{aligned} G_{11} &= \begin{bmatrix} -b_1\mu_{13} & b_1\mu_{12} + b_2\mu_{22} & 0 \\ -b_2\mu_{23} & 0 & 0 \end{bmatrix}, \\ G_{12} &= \begin{bmatrix} -b_1\mu_{13} & 0 & 0 \\ -b_2\mu_{23} & b_1\mu_{12} + b_2\mu_{22} & 0 \end{bmatrix}, \\ G_{21} &= \begin{bmatrix} -b_1\mu_{14} & 0 & b_1\mu_{12} + b_2\mu_{22} \\ -b_2\mu_{24} & 0 & 0 \end{bmatrix}, \\ G_{22} &= \begin{bmatrix} -b_1\mu_{14} & 0 & 0 \\ -b_2\mu_{24} & 0 & b_1\mu_{12} + b_2\mu_{22} \end{bmatrix}. \end{aligned}$$

Assuming that  $\mu_{ik} = \gamma_{ik}\beta^k$ ,  $\mathbf{x}$  is thus asymptotically Gaussian with mean vector given by (33) and covariance matrix given by (34). Note  $A_{ij}$  is a  $2 \times 2$  matrix and  $B_{ijk}^{lp}$  and  $C_{ijk}$  are constants.  $\square$

#### ACKNOWLEDGMENT

The work of LAD is supported by the National Science Foundation (CCF-1422631 and CCF-1453563).

#### REFERENCES

- [1] L. A. Dalton, M. E. Benalcázar, M. Brun, and E. R. Dougherty, "Analytic representation of Bayes labeling and Bayes clustering operators for random labeled point processes," *IEEE Transactions on Signal Processing*, vol. 63, no. 6, pp. 1605–1620, 2015.
- [2] L. Dalton and E. Dougherty, "Intrinsically optimal Bayesian robust filtering," *IEEE Transactions on Signal Processing*, vol. 62, no. 3, pp. 657–670, 2014.
- [3] V. P. Kuznetsov, "Stable detection when the signal and spectrum of normal noise are inaccurately known," *Telecommunications and Radio Engineering*, vol. 30-31, pp. 58–64, 1976.
- [4] S. A. Kassam and T. I. Lim, "Robust Wiener filters," *Journal of the Franklin Institute*, vol. 304, no. 415, pp. 171–185, October/November 1977.
- [5] H. V. Poor, "On robust Wiener filtering," *IEEE Trans. Automatic Control*, vol. 25, no. 4, pp. 531–536, 1980.
- [6] E. R. Dougherty, J. Hua, Z. Xiong, and Y. Chen, "Optimal robust classifiers," *Pattern Recognition*, vol. 38, no. 10, pp. 1520–1532, 2005.
- [7] L. A. Dalton and E. R. Dougherty, "Optimal classifiers with minimum expected error within a Bayesian framework—Part I: Discrete and Gaussian models," *Pattern Recognition*, vol. 46, no. 5, pp. 1301–1314, 2013.
- [8] —, "Optimal classifiers with minimum expected error within a Bayesian framework—Part II: Properties and performance analysis," *Pattern Recognition*, vol. 46, no. 5, pp. 1288–1300, 2013.
- [9] E. R. Dougherty and M. Brun, "A probabilistic theory of clustering," *Pattern Recognition*, vol. 37, no. 5, pp. 917–925, 2004.
- [10] G. Choquet, "Theory of capacities," *Annales de l'institut Fourier*, vol. 5, pp. 131–295, 1954.
- [11] D. G. Kendall, "Foundations of a theory of random sets," *Stochastic Geometry*, vol. 3, no. 9, pp. 322–376, 1974.
- [12] G. Matheron, *Random sets and integral geometry*. New York: John Wiley & Sons, 1975.
- [13] S. N. Chiu, D. Stoyan, W. S. Kendall, and J. Mecke, *Stochastic geometry and its applications*, 3rd ed., ser. Wiley Series in Probability and Statistics. Chichester, West Sussex, United Kingdom: John Wiley & Sons, 2013.
- [14] D. A. Binder, "Bayesian cluster analysis," *Biometrika*, vol. 65, no. 1, pp. 31–38, 1978.
- [15] F. A. Quintana and P. L. Iglesias, "Bayesian clustering and product partition models," *Journal of the Royal Statistical Society: Series B (Statistical Methodology)*, vol. 65, no. 2, pp. 557–574, 2003.
- [16] A. Fritsch, K. Ickstadt *et al.*, "Improved criteria for clustering based on the posterior similarity matrix," *Bayesian analysis*, vol. 4, no. 2, pp. 367–391, 2009.
- [17] M. Meilă, "Comparing clusterings an information based distance," *Journal of multivariate analysis*, vol. 98, no. 5, pp. 873–895, 2007.
- [18] M. H. DeGroot, *Optimal statistical decisions*. Hoboken, NJ: John Wiley & Sons, 2005.
- [19] L. Dalton, V. Ballarin, and M. Brun, "Clustering algorithms: On learning, validation, performance, and applications to genomics," *Current genomics*, vol. 10, no. 6, pp. 430–445, 2009.
- [20] S. Wade and Z. Ghahramani, "Bayesian cluster analysis: Point estimation and credible balls," *arXiv preprint arXiv:1505.03339*, 2015.
- [21] C. Fraley and A. E. Raftery, "Model-based clustering, discriminant analysis, and density estimation," *Journal of the American statistical Association*, vol. 97, no. 458, pp. 611–631, 2002.
- [22] T. B. M. Chris Fraley, Adrian E. Raftery and L. Scrucca, "mclust version 4 for r: Normal mixture modeling for model-based clustering, classification, and density estimation," Department of Statistics, University of Washington, Tech. Rep. Technical Report No. 597, 2012.

- [23] R Core Team, *R: A Language and Environment for Statistical Computing*, R Foundation for Statistical Computing, Vienna, Austria, 2017. [Online]. Available: <https://www.R-project.org/>
- [24] P. Rossi, *bayesm: Bayesian Inference for Marketing/Micro-Econometrics*, 2017, r package version 3.1-0.1. [Online]. Available: <https://CRAN.R-project.org/package=bayesm>
- [25] A. Fritsch, *mcclust: Process an MCMC Sample of Clusterings*, 2012, r package version 1.0. [Online]. Available: <https://CRAN.R-project.org/package=mcclust>
- [26] S. Wade, *mcclust.ext: Point estimation and credible balls for Bayesian cluster analysis*, 2015, r package version 1.0.
- [27] E. R. Dougherty and J. Pelz, "Morphological granulometric analysis of electrophotographic images – size distribution statistics for process control," *Optical Engineering*, vol. 30, pp. 438–445, 1991.
- [28] E. R. Dougherty and F. Sand, "Representation of linear granulometric moments for deterministic and random binary euclidean images," *Visual Communication and Image Representation*, vol. 6, pp. 69–79, 1995.
- [29] F. Sand and E. R. Dougherty, "Robustness of granulometric moments," *Pattern Recognition*, vol. 32, no. 9, pp. 1657–1665, 1999.
- [30] —, "Asymptotic granulometric mixing theorem: Morphological estimation of sizing parameters and mixture proportions," *Pattern Recognition*, vol. 31, pp. 53–61, 1998.
- [31] K. Sivakumar, Y. Balagurunathan, and E. R. Dougherty, "Asymptotic joint normality of the granulometric moments," *Pattern Recognition Letters*, vol. 22, pp. 1537–1543, 2001.
- [32] H. Cramér, "Mathematical methods of statistics," Princeton, NJ, 1947.